J. Math. Biol. (2015) 70:805–828
DOI 10.1007/s00285-014-0782-y

Mathematical Biology

Post-transcriptional regulation in the nucleus and cytoplasm: study of mean time to threshold (MTT) and narrow escape problem

D. Holcman · K. Dao Duc · A. Jones · H. Byrne · K. Burrage

Received: 19 July 2013 / Revised: 11 March 2014 / Published online: 8 April 2014

Abstract Messenger RNAs (mRNAs) can be repressed and degraded by small non-coding RNA molecules. In this paper, we formulate a coarsegrained Markov-chain description of the post-transcriptional regulation of mRNAs by either small interfering RNAs (siRNAs) or microRNAs (miRNAs). We calculate the probability of an mRNA escaping from its domain before it is repressed by siRNAs/miRNAs via calculation of the mean time to threshold: when the number of bound siRNAs/miRNAs exceeds a certain threshold value, the mRNA is irreversibly repressed. In some cases, the analysis can be reduced to counting certain paths in a reduced Markov model. We obtain explicit expressions when the small RNA bind irreversibly to the mRNA and we also discuss the reversible binding case. We apply our models to the study of RNA interference in the nucleus, examining the probability of mRNAs escaping via small nuclear pores before being degraded by siRNAs. Using the same modelling framework, we further investigate the effect of small, decoy RNAs (decoys) on the process of post-transcriptional regulation, by studying regulation of the tumor suppressor gene, *PTEN*: decoys are able to block binding sites on *PTEN* mRNAs, thereby

D. Holcman (✉) · K. Dao Duc
Applied Mathematics and Computational Biology, IBENS, Ecole Normale Supérieure, 46 rue d'Ulm, 75005 Paris, France
e-mail: david.holcman@ens.fr

A. Jones
Computational Biology Group, Department of Computer Science, University of Oxford, Wolfson Building, Parks Rd, Oxford OX1 3QD, UK

H. Byrne
Oxford Centre for Collaborative and Applied Mathematics, Mathematical Institute, University of Oxford, 24-29 St Giles', Oxford OX1 3LB, UK

K. Burrage (✉)
School of Mathematical Sciences, Queensland University of Technology, Brisbane, Australia
e-mail: kevin.burrage@gmail.com

reducing the number of sites available to siRNAs/miRNAs and helping to protect it from repression. We calculate the probability of a cytoplasmic *PTEN* mRNA translocating to the endoplasmic reticulum before being repressed by miRNAs. We support our results with stochastic simulations.

Keywords Stochastic process · Markov chain · Gene expression · mean first passage time · Fokker Planck equation · PTEN · mRNA

Mathematics Subject Classification (2010) 92B05 · 60J28 · 60J70

1 Introduction

Gene expression is the process by which genes are transcribed into messenger RNA (mRNA) molecules which are in turn translated into proteins. Gene regulatory networks consist of groups of genes whose functions can be positively or negatively affected by various signals and/or molecular interactions, which promote or inhibit the production of proteins (Alberts 1998). In this study, we focus on post-transcriptional (or translational) regulation by small RNAs. Post-transcriptional regulation occurs between the transcription and translation of a gene (Alberts 1998). There are many types of post-transcriptional regulation, and nearly all genes can be controlled in this way. We focus on two types of post-transcriptional regulation: RNA interference (RNAi) (Alberts 1998), and post-transcriptional regulation of the tumour suppressor gene, *PTEN* (Sumazin et al. 2011). In particular, the *PTEN* process was chosen because of the important role *PTEN* plays in the prevention of tumourigenesis, as explained in Sect. 1.2. As we shall see in Sect. 2.1, both processes can be modelled by the same general framework, which we present in terms of the *PTEN* problem. Formulation of the RNAi problem as a particular case of the general model is presented in Sect. 2.2. We present the results of our stochastic simulations in Sect. 3, and conclude in Sect. 4 with a discussion of our results and ideas for future work. First, let us introduce the biological motivation behind each problem.

1.1 RNA interference in the nucleus

In eukaryotes, mRNA transcription occurs within the nucleus. Once transcribed, mRNAs form complexes with proteins, and are dispersed throughout the nucleus as they move by Brownian motion (Vargas et al. 2005). They subsequently exit the nucleus via small pores on the surface of the nucleus, roughly 120 nm in diameter, to be translated into protein in the cytoplasm (Grunwald et al. 2010). RNA interference (RNAi) is a biological process in which this gene expression is regulated via interactions between small RNA molecules, known as small interfering RNA (siRNA), and specific target mRNA molecules (Alberts 1998). The siRNAs are initially formed of two ∼22-nucleotide strands of RNA, but are subsequently cleaved into two individual strands, one of which is incorporated into the RNA-induced silencing complex (RISC). Once an siRNA binds to an mRNA target, the mRNA is degraded by Argonaute (Ago), the catalytic component of RISC.

A recent study by Robb et al. (2005) revealed a new role for RNAi in nuclear post-transcriptional regulation, by demonstrating siRNA-induced, RNAi-mediated degradation of target mRNAs in the nucleus of HeLa cells. This process results in down-regulation of target genes, as the number of target transcripts that reach the translation machinery in the cytoplasm is reduced. Additionally, Paul et al. (2002) reported the existence of nuclear post-transcriptional regulation, with results that support the hypothesis of Robb et al. that certain siRNAs can suppress mRNAs before they are able to exit the nucleus for translation in the cytoplasm (Robb et al. 2005; Paul et al. 2002). We formulate this process in terms of a narrow escape problem, as an mRNA diffusing in the nucleus, bounded by the nuclear membrane save for a few small nuclear pores, and study the probability of an mRNA escaping into the cytoplasm via a nuclear pore before it is bound to and degraded by siRNAs (Schuss et al. 2007).

1.2 Post-transcriptional regulation of *PTEN* in the cytoplasm

In addition to RNAi, we also study post-transcriptional control of the tumor suppressor gene, *PTEN*. *PTEN* plays an important role in the prevention of tumor initiation and progression by promoting apoptosis (Salmena and Carracedo 2008). Translation of an mRNA begins in the cytoplasm via binding of "free" ribosomes to the mRNA. When a protein is destined for cell secretion, its polypeptide chain contains a short sequence of amino acids known as the endoplasmic reticulum (ER)-targeting signal sequence (Alberts et al. 2008). If an ER-targeting signal sequence is read by a ribosome, it facilitates the transport of the mRNA, and the partially-translated protein, to the rough ER, where translation of the protein continues. Once fully translated, the protein is secreted to the recipient cell, while the mRNA remains bound to the ER for further translation (Alberts et al. 2008). Putz et al. (2012) demonstrated that the PTEN protein, commonly localised in the cytoplasm and nucleus of a cell, is also secreted from the cell. From this, we assume in our models that if a *PTEN* mRNA binds to a ribosome, it localizes to the ER and, once it is bound at the ER, it remains bound.

By a similar mechanism to RNAi, *PTEN* is post-transcriptionally regulated via binding of small RNA molecules, known as microRNAs (miRNAs), to the $3'$-untranslated region (UTR) of its mRNA (Sumazin et al. 2011). In contrast to siRNA-mRNA binding, miRNA-mRNA binding is thought to primarily result in repression of mRNA translation, although mRNA degradation has also been observed (Jackson and Standart 2007). In the model developed below we will assume that binding by an miRNA results in permanent translational repression of the mRNA.

As reported by Sumazin et al. (2011), an assortment of modulation mechanisms can affect this regulation of *PTEN* by miRNAs. One such mechanism occurs when binding sites are blocked, preventing miRNAs from binding to their targets. In 2010, Eiring et al. suggested that specific decoy RNAs ("decoys") can achieve this by binding to the same sites as miRNAs, thereby interfering with miRNA-mRNA interactions. If these decoys block the binding sites of *PTEN* mRNAs, then *PTEN* will be up-regulated as there will be fewer opportunities for miRNAs to bind and repress *PTEN* translation. A schematic is shown in Fig. 1.

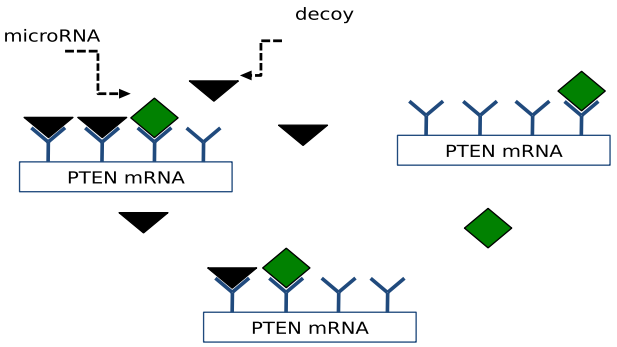

Fig. 1 A schematic of the miRNA-*PTEN* post-transcriptional regulatory process, with miRNAs and decoys competing for binding to *PTEN* mRNA

Again, we formulate this process in terms of a narrow escape problem (Schuss et al. 2007; Holcman et al. 2004): an mRNA molecule is confined to the cytoplasm by the cell membrane, save for a few small, stationary targets (ribosomes) via which the particle can escape into the ER. In our model we assume that the time for translocation of an mRNA to the ER is negligible, and that, if an mRNA comes into contact with a ribosome before it is repressed, it is irreversibly removed from the system (representing instantaneous and permanent removal to the ER). We also assume that ribosomal diffusion is negligible compared to mRNA diffusion. We study the probability of an mRNA binding to a ribosome, and subsequently translocating (escaping) to the ER, before it is repressed by miRNAs.

1.3 Mean time to threshold

Cooperativity of siRNAs/miRNAs can be defined as the repression of a target as a result of the positive interaction between two or more siRNAs/miRNAs in the same 3′UTR (Broderick et al. 2011). In particular, for the *PTEN* problem, a study by Xiao et al. (2008) suggested a potential cooperativity between miR-17-5p and miR-19 in the repression of *PTEN* (Xiao et al. 2008). Broderick et al. (2011) suggested at least three distinct regulatory mechanisms (see Fig. 2) that could account for the increase in target repression of mRNAs containing multiple binding sites (Broderick et al. 2011):

1. **Cooperative binding**—Binding of an siRNA/miRNA-Ago complex to a site increases the affinity of a second complex to an adjacent site. Silencing of the transcript may arise from interactions between adjacent Ago proteins.
2. **Cooperative function**—Multiple siRNA/miRNA-Ago complexes bind to a target independently of one another, but the interaction of one complex could recruit binding proteins that repress the target. Along with an increase in the number of complexes bound, there would be also be an increase in the likelihood of repressive factors being recruited to the mRNA.
3. **Multiple, independent sites**—Each siRNA/miRNA-Ago complex functions independently, but as the number of binding sites increases, the probability of a complex locating a site increases.

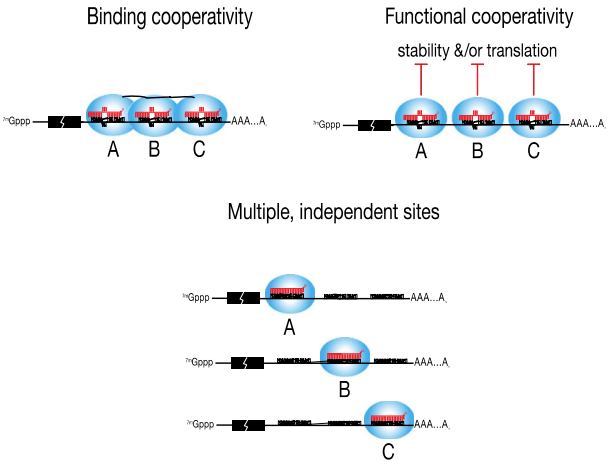

Fig. 2 Three potential regulatory mechanisms that could account for the increased repression activity observed in target transcripts containing multiple siRNA/miRNA binding sites (see main text for details). **a** Cooperative binding, **b** cooperative function, **c** multiple, independent sites (Broderick et al. 2011)

Using this idea of cooperativity, we analyse the probability of mRNA repression by siRNAs/miRNAs by examining the mean time to threshold (MTT) of the number of bound siRNAs/miRNAs.

2 Model formulation

In this section, we present a general framework to estimate the probability, P_a, of an mRNA reaching a small target before it is repressed by miRNAs/siRNAs. We use a stochastic modelling approach to account for the small number of mRNAs and binding sites for siRNAs/miRNAs. In the case of RNAi in the nucleus, P_a represents the probability that the mRNA physically translocates outside the nucleus via a nuclear pore before degradation. In the case of *PTEN* regulation in the cytoplasm, P_a corresponds to binding of an mRNA to a ribosome for translocation to the ER before irreversible translational repression.

In Sect. 2.1, we present the two-dimensional Markov Chain model for *PTEN* regulation in the cytoplasm. In Sect. 2.2, we use Markov Chain analysis to explicitly compute the escape probability for the one-dimensional model of RNAi in the nucleus.

2.1 General model framework for post-transcriptional regulation of *PTEN*

In this section, we formulate a model for the safe delivery of a *PTEN* mRNA to the ER, via binding to a ribosome (represented by a small, stationary target within the cytoplasm). We assume that mRNAs have binding sites which are complementary to two types of small RNAs: miRNAs, s, that are capable of repressing the mRNA, and decoys, d, that can protect the mRNA from repression by blocking the binding sites. We assume that when a decoy is bound to a site, no miRNA can bind to that same site,

and vice versa. In general, miRNAs and decoys compete for the same binding sites, and we will consider both reversible and irreversible binding to these sites. When the number of miRNAs bound to an mRNA exceeds a certain threshold, T, the mRNA is considered to be irreversibly repressed.

In general, we consider that all small RNAs are freely diffusing, with diffusion coefficient, D_s, in a confined domain, and are present in large proportion compared to the number of mRNAs (Ragan et al. 2011). The mRNAs are modelled as diffusing particles with a diffusion coefficient, D_m. The diffusion coefficient for the small RNAs is such that $D_s \gg D_m$ (Morozova et al. 2012). Each mRNA has a finite and small number of binding sites, N_b (assumed to be in the range of 10–20). The *PTEN* model assumes that these interactions between the mRNA, miRNA and decoys are taking place in are taking place in the cytoplasm. The parameters for both this model and the RNAi model are summarized below.

Parameter	Description
τ	Mean time of mRNA to a pore/target
k_f	Forward binding rate of small RNAs to an mRNA
k_b^s	Unbinding rate of siRNAs/miRNAs, s
k_b^d	Unbinding rate of decoys, d
N_b	Total number of binding sites on a single mRNA
T	Threshold number of bound miRNAs/siRNAs required for mRNA repression

The motion of an mRNA, $\boldsymbol{x}(t)$, in a confined domain, Ω, is described by the Brownian dynamics

$$d\boldsymbol{x} = \sqrt{2}\boldsymbol{B}(\boldsymbol{x})\, d\boldsymbol{w}(t), \tag{1}$$

where $\boldsymbol{B}(\boldsymbol{x})$ is a diffusion tensor, and $\boldsymbol{w}(t)$ is a vector of independent standard Brownian motions (Holcman et al. 2012). The state of each mRNA can be described by the probability density function

$$Pr\{\boldsymbol{x}(t) \in \boldsymbol{x} + d\boldsymbol{x}, s(t) = s, d(t) = d\} = p_{s,d}(\boldsymbol{x}, t)d\boldsymbol{x}, \tag{2}$$

which represents the probability that an mRNA is found at position $\boldsymbol{x}$ at time t with s miRNAs and d decoys bound. When the number of bound miRNAs, s, reaches a threshold, T, the mRNA is repressed. For N small targets, of radius $\varepsilon \ll 1$, in the interior the domain, the narrow escape problem can be formulated as a mixed Dirichlet-Neumann boundary value problem (BVP) (Cheviakov et al. 2010), with boundary conditions

$$p_{s,d}(\boldsymbol{x}, t) = 0 \quad \text{for } \boldsymbol{x} \in \partial\Omega_a \tag{3}$$

$$\frac{\partial \boldsymbol{B}\boldsymbol{B}^T(\boldsymbol{x}) p_{s,d}}{\partial \boldsymbol{n}(\boldsymbol{x})}(\boldsymbol{x}, t) = 0 \quad \text{for } \boldsymbol{x} \in \partial\Omega_r. \tag{4}$$

where $0 \leq s \leq T, s + d \leq N_b$, and $\boldsymbol{n}(\boldsymbol{x})$ is the outward unit normal on $\boldsymbol{x} \in \partial\Omega_r$. Condition (3) states the assumption that, for $j = 1, \ldots, N$, if an mRNA arrives at the surface of the j-th target, $\partial\Omega_{\varepsilon_j}$, where $\partial\Omega_a = \cup_{j=1}^{N} \partial\Omega_{\varepsilon_j}$ is the total surface area occupied by all pores, then it will leave the domain almost surely, i.e., with probability one. Condition (3) is the zero-flux boundary condition for the rest of the domain, $\partial\Omega_r = \partial\Omega - \partial\Omega_a$.

2.1.1 Master–Fokker–Planck equation

The joint probability density function (Jpdf) is the solution of a Master–Fokker–Planck equation (Schuss 2010) that we shall formulate now. For $0 < s < T$ and $0 < d < N_b$, it is given by

$$\begin{aligned}\frac{\partial}{\partial t} p_{s,d}(\boldsymbol{x}, t) = & \, div(\boldsymbol{B}\boldsymbol{B}^T(\boldsymbol{x}) \nabla p_{s,d}(\boldsymbol{x}, t)) - 2k_f(N_b - s - d) p_{s,d}(\boldsymbol{x}, t) \\ & - (k_b^s s + k_b^d d) p_{s,d}(\boldsymbol{x}, t) + k_b^s (s+1) p_{s+1,d}(\boldsymbol{x}, t). \\ & + k_b^d (d+1) p_{s,d+1}(\boldsymbol{x}, t) + k_f(N_b - s - d + 1) p_{s-1,d}(\boldsymbol{x}, t) \\ & + k_f(N_b - s - d + 1) p_{s,d-1}(\boldsymbol{x}, t). \end{aligned} \tag{5}$$

Here, we make the assumption that s and d are abundant in the cytoplasm, such that binding does not affect their total amount in the cytoplasm (Ebert 2010). The Markov Eq. (44) has been derived in the classical approximation where we considered that during the time interval $[t, t + \Delta t]$, if there are already s and d bound miRNAs and decoys, respectively, an miRNA or decoy can bind with rate $k_f(N_b - s - d)\Delta t$. A miRNA (or decoy) can unbind with rate $k_b^s s \Delta t$ (or $k_b^d d \Delta t$). A more detailed description of the derivation of the Jpdf is given in Dao Duc and Holcman (2010). The mathematical difficulty and novelty here is to examine the master equations at the reaction boundaries: when the number of bound miRNAs is equal to the threshold T, the mRNA is repressed and we assume that the rate of return from the state $s = T$ to any previous state is zero. This is modeled as an absorbing boundary condition to repression: for all time, t, and for all d, $p_{T+1,d}(t) = 0$. Similarly, we assume there are no transitions to or from negative states, i.e., $p_{s,d} = 0$ for $s < 0$ or $d < 0$, and that the maximum number of possible bindings is N_b, i.e., $p_{s,d} = 0$ for $s + d > N_b$. The master equations associated with these boundary conditions are detailed in Appendix A.

The transition diagram is summarized in Fig. 3. The general system of equations cannot, in general, be solved analytically. However we can compute various quantitites asymptotically or via the stochastic simulation algorithm (SSA) (Gillespie 1977). Quantitites of interest include the probability that an mRNA escapges to the ER (by locating a ribosome) before it is repressed (see Fig. 9a).

2.1.2 Reduction of the Master–Fokker–Planck to a Markov chain

To estimate the probability of an mRNA exiting the domain before repression, we integrate the Master-Fokker-Planck equations over the domain, Ω (*n.b.* unless stated otherwise, we assume that the subscript $\{s, d\}$ represents that there are s miRNAs and

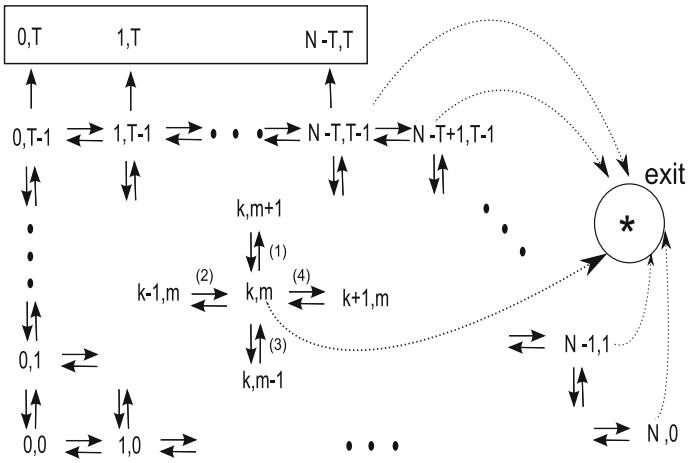

Fig. 3 Markov chain diagram for the mRNA state. The general transitions are represented in the inner diagram, while we emphasize the boundary condition. The rectangle represents the state where the mRNA is repressed (absorbing state). From each non absorbing state, there is also a probability to exit, represented in the diagram as *asterisk*

d decoys bound to the mRNA, with $s \in [|0, T|]$ and $d \in [|0, N_b - s|])$. The survival probability of a particle at time t is given by

$$p^S_{s,d}(t) = \int_\Omega p_{s,d}(\boldsymbol{x}, t) d\boldsymbol{x}, \tag{6}$$

which is the probability of an mRNA being found intact within the domain at time t given any initial position, x, in the domain, Ω. From this, we define the conditional outflux probability as

$$J_{s,d}(t) = \oint_{\partial\Omega_a} \frac{\partial \boldsymbol{B}(\boldsymbol{x}) \boldsymbol{B}^T(\boldsymbol{x}) p_{s,d}}{\partial \boldsymbol{n}} (\boldsymbol{x}, t) dS_{\boldsymbol{x}}, \tag{7}$$

which represents the instantaneous arrival rate of an mRNA to a target. Binding to targets is rare as targets occupy only a small fraction of the domain. Therefore, the flux can be approximated in the small hole limit as (Schuss et al. 2007)

$$J_{s,d}(t) = \frac{1}{\tau} p^S_{s,d}(t), \tag{8}$$

where τ is the mean arrival time of an mRNA to a target. This mean first passage time (MFPT) does not depend on the number of bound miRNAs/decoys, but does depend on the diffusion properties of the mRNA and the number of targets. For constant isotropic diffusion, τ has been calculated for various geometries and binding site configurations. The details of these formulas are recalled in Appendix B. The formulas are used below where they are compared with stochastic simulations. The survival probability, given

by (6), of an mRNA being found intact in the domain at time t, satisfies the general CME Dao Duc and Holcman (2010),

$$\begin{aligned}\frac{\partial}{\partial t}p^S_{s,d}(t) = &-\frac{1}{\tau}p^S_{s,d}(t) - 2k_f(N_b - s - d)p^S_{s,d}(t) - (k^s_b s + k^d_b d)p^S_{s,d}(t)\\ &+ k^s_b(s+1)p^S_{s+1,d}(t) + k^d_b(d+1)p^S_{s,d+1}(t)\\ &+ k_f(N_b - s - d + 1)p^S_{s-1,d}(t) + k_f(N_b - s - d + 1)p^S_{s,d-1}(t).\end{aligned}$$

The boundary terms are obtained similarly to those derived in Appendix A, by integrating over the domain, Ω.

The first time, $\bar{\tau}^T$, that the number of bound miRNAs reaches the threshold, T, is known as the "mean time to threshold" (MTT). It allows us to define the escape probability P_a that the mRNA escapes before it is repressed. Similarly, we can define the probability that an mRNA is repressed before it escapes as P_d. The probability that an mRNA exits the domain before it is repressed is the sum over all probabilities that there are $s < T$ bound miRNAs when an mRNA reaches a target at time, t, that is,

$$P_a(t) = \sum_{s=0}^{T-1}\frac{1}{\tau}p^S_{s,d}(t) + \sum_{d=N_b-T+1}^{N_b}\sum_{s=0}^{N_b-d}p^S_{s,d}(t). \tag{9}$$

The overall exit probability for an intact mRNA is

$$P_a = \int_0^\infty P_a(t)dt. \tag{10}$$

Similarly, the probability of an mRNA being repressed before it escapes can be defined as

$$P_d = \sum_{k=0}^{N_b-T}\sum_{d=0}^{N_b-T}p^S_{T,k}(\infty), \tag{11}$$

where

$$p^S_{T,d}(\infty) = \lim_{t\to\infty}p^S_{T,d}(t). \tag{12}$$

Combining (9) and (10), and using the conservation of probability, we can re-formulate this as

$$P_a = \sum_{s=0}^{T-1}\sum_{d=0}^{N_b-T}\int_0^\infty J_{s,d}(r)dr + \sum_{d=N_b-T+1}^{N_b}\sum_{s=0}^{N_b-d}\int_0^\infty J_{s,d}(r)dr. \tag{13}$$

In the small hole approximation, the exit time is Poissonian (Schuss et al. 2007). To estimate the survival probability, we integrate the Markov chain over the domain, Ω, and simplify our results by defining

$$a_{s,d} = \int_0^\infty p^S_{s,d}(t)dt, \tag{14}$$

which represents the probability of an mRNA being found intact within the domain at any time. From this, (13) can be written as

$$P_a = \frac{1}{\tau}\sum_{s=0}^{T-1}\sum_{d=0}^{N_b-T} a_{s,d} + \frac{1}{\tau}\sum_{d=N_b-T+1}^{N_b}\sum_{s=0}^{N_b-d} a_{s,d}. \tag{15}$$

The probability $a_{s,d}$ satisfies

$$\begin{aligned} 0 = &-\frac{1}{\tau}a_{s,d} - 2k_f(N_b - s - d)a_{s,d} - (k_b^s s + k_b^d d)a_{s,d} \\ &+ k_b^s(s+1)a_{s+1,d} + k_b^d(d+1)a_{s,d+1} \\ &+ k_f(N_b - s - d + 1)a_{s-1,d} + k_f(N_b - s - d + 1)a_{s,d-1}, \end{aligned} \tag{16}$$

for $0 < s < T$ and $0 < d < N_b - T$. This results from

$$\lim_{t\to\infty} p^S_{s,d}(t) = 0, \quad \text{for } s \neq T, \tag{17}$$

in that, the probability to find the mRNA inside the cytoplasm is zero except in the following cases:

$$\begin{aligned} p_{T,d}(\infty) &= k_f(N_b - T - d + 1)a_{T-1,d}, \text{ where } N_b - T > d \geq 0 \\ p_{T,N_b-T}(\infty) &= k_f a_{T-1,N_b-T}, \end{aligned}$$

which corresponds to the probability of mRNA repression at $t = \infty$. For $s = 0$ and $d = 0$, we further obtain the boundary conditions,

$$-1 = -\frac{1}{\tau}a_{0,0} - 2k_f N_b a_{0,0} + k_b^s a_{1,0} + k_b^d a_{0,1} \tag{18}$$

$$0 = -\frac{1}{\tau}a_{0,N_b} - k_b^d N_b a_{0,N_b} + k_f a_{0,N_b-1}, \tag{19}$$

using (17) and the initial condition,

$$p_{0,0}(0) = 1.$$

Thus we have the following set of conditions. For $N_b > d > 0$,

$$\begin{aligned} 0 = &-\frac{1}{\tau}a_{0,d} - 2k_f(N_b - d)a_{0,d} - k_b^d d a_{0,d} + k_b^s a_{1,d} \\ &+ k_b^d(d+1)a_{0,d+1} + k_f(N_b - d + 1)a_{0,d-1}. \end{aligned}$$

For $T-1 > s > 0$,

$$0 = -\frac{1}{\tau}a_{s,0} - 2k_f(N_b - s)a_{s,0} - k_b^s s a_{s,0} + k_b^s(s+1)a_{s+1,0} + k_b^d a_{s,1} + k_f(N_b - s + 1)a_{s-1,0}.$$

For $s = T - 1$, $N_b - T > d > 0$,

$$0 = -\frac{1}{\tau}a_{T-1,d} - 2k_f(N_b - T + 1 - d)a_{T-1,d} - (k_b^s(T-1) + k_b^d d)a_{T-1,d} + k_b^d(d+1)a_{T-1,d+1} + k_f(N_b - T - d + 2)a_{T-2,d} + k_f(N_b - T - d + 2)a_{T-1,d-1}.$$

For $T > s > 0$, $N_b - s = d$,

$$0 = -\frac{1}{\tau}a_{s,N_b-s} - (k_b^s s + (N_b - s)k_b^d)a_{s,N_b-s} + k_f a_{s-1,N_b-s} + k_f a_{s,N_b-s-1}.$$

Using the stochastic simulation algorithm, we simulate the number of bound decoys and miRNAs on a single mRNA (Fig. 6), for particular values of the reversible and irreversible binding rates.

2.1.3 Computing the escape probability P_a

Irreversible binding $k_b^s = k_b^d = 0$

In the irreversible case ($k_b^s = k_b^d = 0$), we can compute the survival probability using the method of DaoDuc and Holcman (2010), namely by summing probabilities over all trajectories starting from (0,0) and leading to the repression state (T,m). We start by considering the path σ with n bindings ($T \le n \le N_b$) for which the associated probability is

$$P(\sigma) = \left(\frac{1}{2}\right)^n \prod_{i=0}^{n-1} \frac{k_f(N_b - i)}{k_f(N_b - i) + 2/\tau}. \tag{20}$$

The number of these paths of length n is then $\binom{n-1}{T-1}$, since there are T bindings with miRNAs including the last one. Thus, the probability of repression before exit, P_d, is given by

$$P_d = \sum_{k=T}^{N_b} \binom{k-1}{T-1} \left(\frac{1}{2}\right)^k \prod_{i=0}^{k-1} \frac{k_f(N_b - i)}{k_f(N_b - i) + 2/\tau}. \tag{21}$$

We use Formula (21) in Fig. 7 to plot and compare P_a as a function of T with stochastic simulations and observe good agreement for different values of τk_f. When the exit

time is large compared with the binding time ($\tau \gg 1/k_f$), we can approximate $\frac{k_f(N_b-i)}{k_f(N_b-i)+2/\tau} = \frac{1}{1+2/(\tau k_f(N_b-i))} \approx 1$ in (21) and thus obtain

$$P_d \approx \sum_{k=T}^{N_b} \binom{k-1}{T-1} \frac{1}{2^k}, \tag{22}$$

which can indeed be interpreted in the following way: neglecting the probability to exit (as τ the mean time to exit is large compared to the mean binding time $1/(k_f(N_b-i))$ to either a decoy or miRNA), the Markov chain converges to a steady state distribution where the number of bound decoys is binomial with parameters $(N_b, 1/2)$. Thus, the probability of repression is given by (22).

Reversible binding

In general, when there are both miRNAs and decoys with reversible binding, the escape probability cannot be resolved analytically. However, using the stochastic simulation algorithm, we obtain the escape probability, as shown in Fig. 9. The simulation in Fig. 9 reveals that the formula obtained in the irreversible case (red line) can be used to approximate the escape probability for small values of τ (until $\tau k_f = 1$).

Now that we have presented the two-dimensional model for*PTEN* post-transcriptional regulation, let us introduce the one-dimensional model for RNAi in the cytoplasm.

2.2 The RNAi model ($d = k_b^d = 0$)

We consider the case that there are no decoys in the system, which we study via the process of RNAi in the nucleus.

2.2.1 Re-formulation of the probability density function

We present a model for the escape of an mRNA from the nucleus via small nuclear pores before being degraded by siRNAs. The model accounts for multiple siRNA binding sites on the mRNA. When the number of siRNAs, S, bound to an mRNA exceeds a given threshold, T, the mRNA is considered to be degraded. When an siRNA occupies a site, no other siRNA can bind. We assume that siRNAs are freely diffusing in the nucleus and that siRNA-mRNA binding is irreversible. We compute the escape probability, P_a, that an mRNA exits the nucleus intact, that is, it escapes through a nuclear pore before there are T siRNAs bound. We characterize the mRNA by (2), with survival probability (6) satisfying the Markov chain (see Fig. 4)

$$\frac{d}{dt}p_s^S(t) = -\frac{1}{\tau}p_s^S(t) - (N_0-s)k_f p_s^S(t) - k_b^s s p_s^S(t) + k_f(N_0-s+1)p_{s-1}^S(t) + k_b^s(s+1)p_{s+1}^S(t),$$

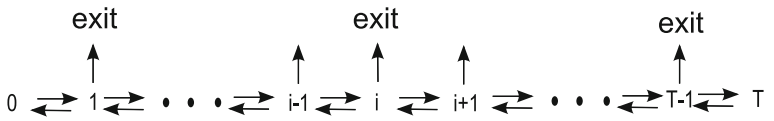

Fig. 4 Markov chain diagram for the mRNA state (no decoys)

with boundary conditions

$$\begin{aligned}\frac{d}{dt}p^S_{T-1}(t) &= -\frac{1}{\tau}p^S_{T-1}(t) - k^s_b(T-1)p^S_{T-1}(t) - k_f(N_0-T+1)p^S_{T-1}(t)\\ &\quad + k_f(N_0-T+2)p^S_{T-2}(t)\\ \frac{d}{dt}p^S_0(t) &= -\frac{1}{\tau}p^S_0(t) - k_f N_0 p^S_0(t) + k^s_b p^S_1(t)\\ \frac{d}{dt}p^S_T(t) &= k_f(N_0-T+1)p^S_{T-1}(t),\end{aligned}$$

using the fact that the transition rate from state T to $T-1$ is zero.

2.2.2 Computing the escape probability, P_a

Irreversible binding

In the irreversible case, $k^s_b = 0$, defining the probability of an mRNA with s siRNAs bound being found intact within the domain at any time, t, as

$$a_s = \int_0^\infty p^S_s(t)dt, \tag{23}$$

the Markov chain simplifies to, for $0 < s < T-1$,

$$0 = -\frac{1}{\tau}a_s - k_f(N_0-s)a_s + k_f(N_0-s+1)a_{s-1}, \tag{24}$$

with $a_T = 0$ and the boundary conditions given by

$$-1 = -\frac{1}{\tau}a_0 - k_f N_0 a_0 \tag{25}$$

$$0 = -\frac{1}{\tau}a_{T-1} - k_f(N_0-T+1)a_{T-1} + k_f(N_0-T+2)a_{T-2} \tag{26}$$

$$p^S_T(\infty) = k_f(N_0-T+1)a_{T-1}.$$

Initially the mRNA is not bound by any siRNAs so $p^V_s(0) = \delta_s$. The escape probability is given by

$$P_a = \frac{1}{\tau}\sum_{k=0}^{T-1} a_s, \tag{27}$$

while the conservation of probability leads to the relation

$$P_a + p_T^S(\infty) = 1. \tag{28}$$

A direct solution of (24) and (25) gives, for $s < T$,

$$a_s = \frac{k_f(N_b - s + 1)}{1/\tau + k_f(N_b - s)} a_{s-1}, \tag{29}$$

where $a_0 = \dfrac{\tau}{1 + k_f N_b \tau}$. Thus,

$$a_s = k_f^k \frac{(N_b)!}{(N_b - s)!} \prod_{j=0}^{s} \frac{1}{1/\tau + k_f(N_b - j)}. \tag{30}$$

Using (27) and (30), the probability that the mRNA escapes the domain intact is given by

$$P_a(T, N_b, x) = \sum_{s=0}^{T-1} x^s \frac{N_b!}{(N_b - s)!} \prod_{j=0}^{s} \frac{1}{1 + (N_b - j)x}, \tag{31}$$

where $x = \tau k_f$. In Fig. 5, we plot the analytical solution of (31) and compare it to simulations obtained with the SSA, for varying values of the parameter $x = \tau k_f$ and the threshold, T. The excellent agreement supports the accuracy of the models and analysis.

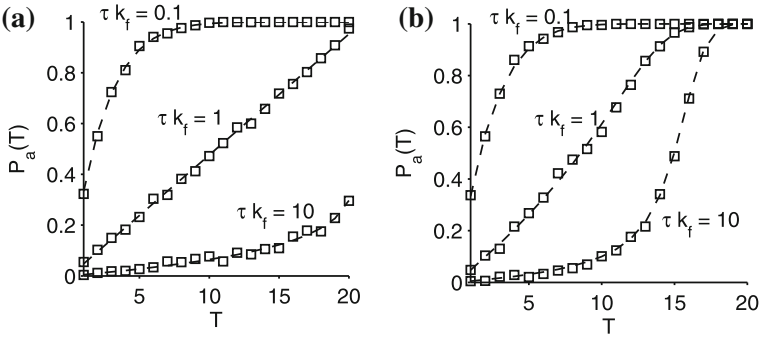

Fig. 5 Escape probability as a function of the threshold T (bound miRNAs) for the RNAi problem (no decoys). **a** Comparison between stochastic simulations (*square*) and analytical Formula (31) (*dotted line*) in the irreversible binding case for different values of $x = \tau = 0.1, 1, 10$. **b** Same as in **a** but with reversible binding case and a comparison with analytical formula (38). For each value of T, we perform 1,000 SSA simulations with $N_b = 20$ and $k_b^s = k_f = 1$

Reversible binding

In the reversible case, the Markov chain is given by

$$\begin{aligned} 0 = &-\frac{1}{\tau}a_s - k_f(N_b - s)a_s - k_b^s s a_s \\ &+ k_b^s(s+1)a_{s+1} + k_f(N_b - s + 1)a_{s-1}, \end{aligned} \tag{32}$$

with boundary conditions given by

$$-1 = -\frac{1}{\tau}a_0 - k_f N_b a_0 + k_b^s a_1 \tag{33}$$

$$\begin{aligned} 0 = &-\frac{1}{\tau}a_{T-1} - k_f(N_b - T + 1)a_{T-1} - k_b^s(T-1)a_{T-1} \\ &+ k_f(N_b - T + 2)a_{T-2} \end{aligned} \tag{34}$$

$$p_T^S(\infty) = k_f(N_b - T + 1)a_{T-1}.$$

We note that (32) can be written as a tridiagonal matrix equation

$$\mathbf{M}\begin{pmatrix} a_0 \\ a_1 \\ \vdots \\ a_{T-1} \end{pmatrix} = \begin{pmatrix} -1 \\ 0 \\ \vdots \\ 0 \end{pmatrix}, \tag{35}$$

where $\mathbf{M}$ is the tridiagonal matrix

$$\mathbf{M} = \begin{pmatrix} \alpha_0 & \beta_1 & 0 & & \dots & 0 \\ \gamma_1 & \alpha_1 & \beta_2 & 0 & (0) & \\ 0 & \ddots & \ddots & \ddots & \ddots & \vdots \\ & \ddots & \ddots & \ddots & \ddots & 0 \\ \vdots & (0) & \ddots & \ddots & \ddots & \beta_{T-1} \\ 0 & \dots & & 0 & \gamma_{T-1} & \alpha_{T-1} \end{pmatrix}, \tag{36}$$

with

$$\begin{aligned} \beta_i &= k_b^s i \\ \gamma_i &= (N_b - i + 1)k_f \\ \alpha_i &= -\left(\frac{1}{\tau} + \beta_i + \gamma_{i+1}\right). \end{aligned} \tag{37}$$

Thus, the probability to reach the threshold, T, is given by

$$P_T = k_f(N_b - T + 1)a_{T-1} = -k_f(N_b - T + 1)m_{T1}^{-1}, \tag{38}$$

where $m_{ij}^{-1} = (\mathbf{M}^{-1})_{ij}$ for $1 \leq i, j \leq T$. A direct computation gives

$$m_{T1}^{-1} = \frac{(-1)^{T+1} \prod_{k=1}^{T-1} \gamma_k}{\theta_T}, \tag{39}$$

where $(\theta_n)_{n\in\mathbb{N}}$ is a sequence satisfying a second order induction relation with polynomial coefficients given by

$$\theta_i = \alpha_{i-1}\theta_{i-1} - \beta_{i-1}\gamma_{i-1}\theta_{i-2}, \tag{40}$$

with $\theta_0 = 1$ and $\theta_1 = \alpha_0$ (Usmani 1994). Using the expressions for α_i, β_i and γ_i, we obtain

$$P_T(\infty) = \frac{k_f^T N_b!}{(N_b - T)! u_T}, \tag{41}$$

where the sequence u_n satisfies, for $i > 1$,

$$u_{i+1} = \left(\frac{1}{\tau} + k_b^s i + k_f(N_b - (i+1) + 1)\right) u_i + k_b^s k_f i (N_b - i + 1) u_{i-1},$$

with $u_0 = -1$ and $u_1 = \frac{1}{\tau} + k_f N_b$. However, the series u_n cannot be obtained explicitly in a simple closed form. As a particular example, $T = 3$ gives

$$P_T(\infty) = \frac{\bar{k_f}^3 N_b(N_b - 1)(N_b - 2)}{Q(\bar{k}_f, \bar{k}_b^s N_b)}, \tag{42}$$

where

$$\begin{aligned} Q(\bar{k}_f, \bar{k}_b^s, N_b) = 1 &+ \bar{k_f} \sum_{0\leq i\leq 2} (N_b - i) + \bar{k_f}^2 \sum_{0\leq i\neq j\leq 2} (N_b - i)(N_b - j) \\ &+ \bar{k_b^s}[3 + 2\bar{k_b^s} + \bar{k_f}(2N_b^2 + 2\bar{k_f} N_b(N_b - 1) + 5N_b - 6)] \\ &+ \bar{k_f}^3 N(N_b - 1)(N_b - 2), \end{aligned}$$

and

$$\bar{k}_f = k_f \tau \text{ and } \quad \bar{k}_b^s = k_b^s \tau. \tag{43}$$

3 Results for RNAi and *PTEN* dynamics

3.1 RNAi

Figure 5b shows the good agreement between the analytical expression (38) and the results of the SSA. Compared with irreversible binding ($k_b^s = 0$), the survival probability is relatively insensitive to the values of the escape time, τ, when τ is small

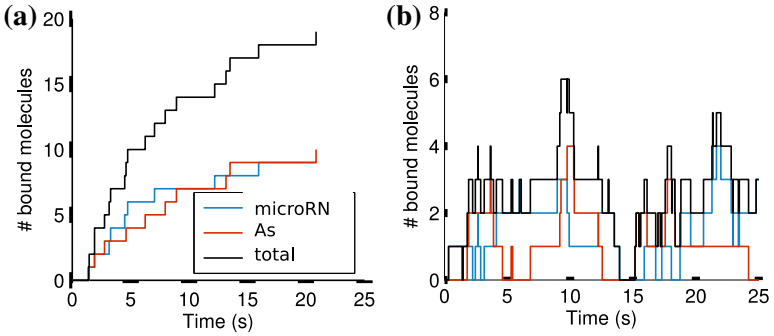

Fig. 6 Stochastic simulation of the dynamics of binding and unbinding to mRNA, for $N_b = 20$, $\tau = 50$s, $k_f = 0.05s^{-1}$ and $T = 10$. **a** Irreversible case. **b** Reversible case with $k_b^s = k_b^d = 0.5s^{-1}$

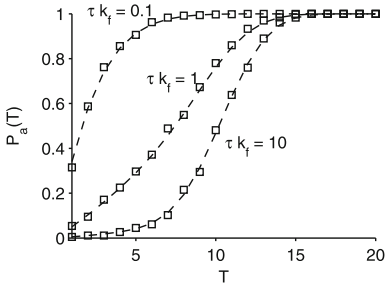

Fig. 7 Escape probability as a function of the threshold T in the irreversible case ($k_b^s = k_b^d = 0$): Formula (21) and the SSA (*square*) agree for several values of τk_f. For each value of T, we perform 1,000 SSA simulations, $N_b = 20$ and $k_f = 1$

compared to the chemical times $\frac{1}{k_b^s}$ and $\frac{1}{k_f}$ (Fig. 5a, b for $\tau k_f = 0.1$). Indeed, when the escape time is short compared to the binding and unbinding times, the miRNAs generally have no time to unbind before the mRNA exits. However, as the escape time, τ, increases, the number of bound miRNAs increases and thus unbinding affects the probability of absorption (Fig. 5a, b for $\tau = 1$ and 10). These changes become apparent for a high threshold value. Thus unbinding can delay the time to reach the threshold, enabling the mRNA to escape with higher probability than in the irreversible case.

3.2 PTEN

In Fig. 6, we use the stochastic simulation algorithm to simulate the number of bound decoys and miRNAs on a single mRNA for varying reversible and irreversible binding rates.

In Fig. 7, we compare $P_a(T)$ obtained from Formula (21) with stochastic simulations. We obtain very good agreement for different values of τk_f.

Figure 8a, c are repetitions of Figs. 5b and 7, respectively, for larger values of the escape time, τ. They show the escape probability as a function of the threshold T (bound miRNAs) for the reversible RNAi problem (no decoys) and the irreversible *PTEN* problem (miRNAs and decoys).

Figure 8b, d show the threshold value, T, as a function of the escape time, τ, for the escape probabilties $P_a = 0.25, 0.5, 0.75$ and 0.95. The red dotted line shows

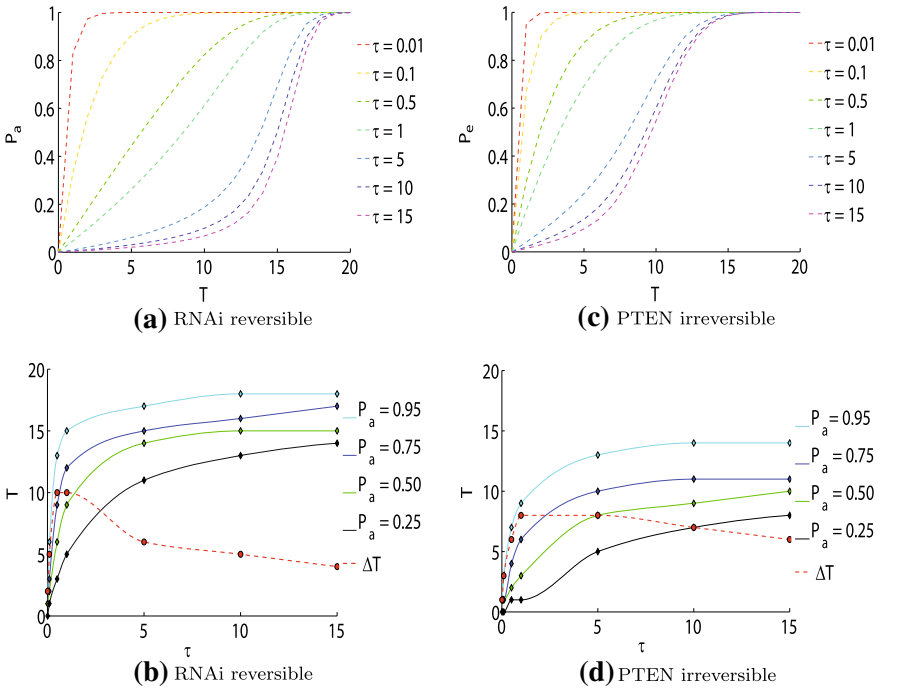

Fig. 8 **a** RNAi reversible, **b** RNAi reversible, **c** PTEN irreversible, **d** *left column* escape probability, P_a, as a function of the threshold, T, for a variety of escape times, τ. *Right column* threshold as a function of escape time for a variety of escape probabilities (*solid lines*), and the change in threshold value, ΔT, from $P_a = 0.25$ to $P_a = 0.95$ (*red dotted line*) (color figure online)

the difference in the threshold required to observe a 95 % probability of escape before repression, i.e., $P_a = 0.95$, compared to the threshold required to observe a 25 % probability of escape before repression, i.e., $P_a = 0.25$, represented by $\Delta T = T(P_a = 0.95) - T(P_a = 0.25)$. This threshold difference is a measure of the steepness of the switch between $P_a \approx 0$ and $P_a \approx 1$ in Fig. 8a, c. A small value of ΔT is representative of an abrupt switch, in which the threshold values for almost certain escape and almost certain repression differ by very little, such that the escape probability depends strongly on the threshold value. A large value of ΔT represents a gradual switch between almost certain escape and almost certain repression, such that the threshold value does not much affect the probability of an mRNA escaping before repression.

In Fig. 8b, when the escape time, τ, is small compared to the forward and backward binding reaction times, $\frac{1}{k_b^i}$ and $\frac{1}{k_f}$, respectively, ΔT is small. This supports the idea that when the escape time is short compared to the forward and backward binding reaction times, the threshold value has almost no effect of the probability of escape, as the miRNAs have generally no time to unbind before the mRNA exits, regardless of the threshold number of miRNA bindings needed for repression. ΔT increases until a maximum at $\tau = 1$, when the escape time and the binding reaction times are equal. This is due to an increase in the number of miRNAs that can bind to an mRNA

before it escapes, as the time spent inside the domain, τ, increases. Thus the threshold number of bound miRNAs needed for repression begins to affect the probability of escape. ΔT then decreases slowly for large τ such that the effect of T on P_a is lessened as the escape time becomes large compared with the binding reaction times. This is because the threshold value is more and more likely to be reached before the mRNA can escape, the longer it remains within the domain. We can see this in Fig. 8a as the switch between $P_a = 0.25$ and $P_a = 0.95$ becomes gradually sharper, meaning that, conversely to $\tau < 1$, the mRNA has a very high probability of being degraded for all but the highest threshold values.

Figure 8d reveals that this effect is also present in the case of decoys with irreversible binding, but to a lesser extent. We see a lower maximum ΔT at $\tau = 1$ and a more gradual decline for $\tau > 1$. This shows that the threshold value has a greater effect on the probability of escape for large τ than for the case of irreversible binding with miRNAs alone. This is most likely due to the introduction of decoys into the system which can block the binding sites of mRNA and are unable to unbind from these sites, making the threshold value harder to reach, even when the mRNA remains in the domain for longer due to a reduced escape time, τ.

The results reported above support those obtained for the case of both decoys and reversible binding, shown in Fig. 9a. For increasing escape time, τ, unbinding events decrease the probability of escape (for intermediate values of T). Dramatic differences appear for a threshold of $T = 11$ and $N_b = 20$ (Fig. 9) leading to a two-fold increase in the probability of escape for the irreversible case ($\approx$0.6) compared to the reversible case ($\approx$0.3). Unbinding of decoys increases the likelihood of the threshold value being reached, and so we observe a decrease in the probability of escape. This effect is hard to predict as both decoys and miRNAs can unbind. Irreversible binding reduces the effect of decoys on the escape probability, and so we see an increase in the effect of T on P_a, similar to that which is observed in the case of reversible binding alone (Fig. 8b). The histogram of the number of bound miRNAs before the mRNA exits is given in Fig. 9b for different values of T.

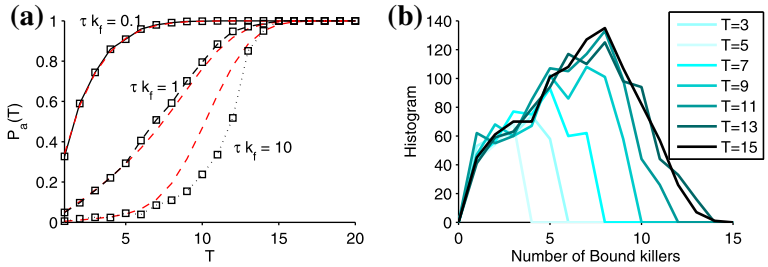

Fig. 9 **a** The escape probability as a function of the threshold, T, of bound miRNAs. Probability of escape (*squares*) for different values of τ in the reversible *PTEN* case, compared to the probability of escape in the irreversible *PTEN* case (*red*) for $N_b = 20$ and $k_f = 1$. **b** Histograms of the number of miRNAs bound to an mRNA before exit for different values of the threshold, T. For each value of T, we perform 1,000 SSA simulations for $N_b = 20$, $k_f = 1$, $k_b^s = k_b^d = 0.5$ (color figure online)

4 Conclusions

We have presented a mathematical framework for studying the stochastic repression of mRNA by siRNAs/miRNAs as a function of elementary parameters such as the threshold to repression, T, the number of binding sites, N_b, and the various kinetics parameters. When the siRNA/miRNA bind reversibly, we found that the probability of escape is decreased compared to irreversible binding. The present approach can be used to obtain precise estimates for the number of siRNAs/miRNAs needed for specific genetic regulation.

By studying the post-transcriptional regulation of PTEN, we have also shown that this behaviour persists when decoys are present. There is, however, another type of molecule that is known to play a role in post-transcriptional regulation of *PTEN*, known as competing endogenous RNA (ceRNA), or 'sponges'. It has been proposed in several studies (e.g., Ebert et al. 2007; Poliseno et al. 2010), and experimentally validated in several others (e.g., Sumazin 2011; Tay et al. 2011), that RNAs that share miRNA binding sites may compete for a shared pool of miRNA. This group of sponge modulators act by soaking up miRNAs, leaving fewer miRNAs to bind to their intended target mRNA. This causes an up-regulation in translation of the target gene, as translational repression is down-regulated. One confirmed sponge, discovered by Poliseno et al. in (2010), is the *PTEN* pseudogene, *PTENP1*. Inclusion of sponge modulation is just one possible extension of the current model that we will explore in future work.

Finally, it is well known that the behaviour of molecules in a cell depends not only on the number of molecules present, but also on the distribution of these molecules within the cell and how they move and interact with each other (Alberts 1998). Processes such as target binding by an siRNA/miRNA may be spatially-dependent; an siRNA/miRNA may find its target site faster, or slower, depending on its initial distance from the target and the mechanism by which it moves through the cell. We are currently developing a spatial model of the system, and will use this to study how subcellular heterogeneity affects the probability of mRNA escape before repression by direct comparison with the models developed in this study.

Appendix A

We shall present here the two-dimensional chemical Markov equations (CME) in the variables s and d introduced in Sect. 2.1. We need to examine carefully the expressions at the boundary of two-dimensional state space around s = T and s = 0 to incorporate the appropriate modifications in the transition rates.

The CME for no bound miRNAs or decoys ($s = d = 0$)

As there are no transitions from negative states, the CME is

$$\frac{\partial}{\partial t} p_{0,0}(\boldsymbol{x}, t) = div(\boldsymbol{B}\boldsymbol{B}^T(\boldsymbol{x})\nabla p_{0,0}(\boldsymbol{x}, t)) - 2k_f N_b p_{0,0}(\boldsymbol{x}, t) + k_b^s p_{1,0}(\boldsymbol{x}, t) + k_b^d p_{0,1}(\boldsymbol{x}, t).$$

The CME for either no bound miRNAs or no bound decoys ($s = 0$ or $d = 0$)

When there are no miRNAs bound, that is, $s = 0$ and $N_b > d > 0$, we have

$$\begin{aligned}\frac{\partial}{\partial t}p_{0,d}(\boldsymbol{x},t) = div(\boldsymbol{B}\boldsymbol{B}^T(\boldsymbol{x})\nabla p_{0,d}(\boldsymbol{x},t)) - 2k_f(N_b-d)p_{0,d}(\boldsymbol{x},t)\\ - k_b^d d p_{0,d}(\boldsymbol{x},t) + k_b^s p_{1,d}(\boldsymbol{x},t) + k_b^d(d+1)p_{0,d+1}(\boldsymbol{x},t)\\ + k_f(N_b-d+1)p_{0,d-1}(\boldsymbol{x},t).\end{aligned}$$

Similarly, for $T-1 > s > 0$ and $d = 0$ (no decoys bound),

$$\begin{aligned}\frac{\partial}{\partial t}p_{s,0}(\boldsymbol{x},t) = div(\boldsymbol{B}\boldsymbol{B}^T(\boldsymbol{x})\nabla p_{s,0}(\boldsymbol{x},t)) - 2k_f(N_b-s)p_{s,0}(\boldsymbol{x},t) - k_b^s s p_{s,0}(\boldsymbol{x},t)\\ + k_b^s(s+1)p_{s+1,0}(\boldsymbol{x},t) + k_b^d p_{s,1}(\boldsymbol{x},t)\\ + k_f(N_b-s+1)p_{s-1,0}(\boldsymbol{x},t).\end{aligned}$$

The CME near the threshold number of bound miRNAs ($s = T-1$)

For $s = T-1$, $d = 0$ (no transition rate from $P_{T,0}$), then

$$\begin{aligned}\frac{\partial}{\partial t}p_{T-1,0}(\boldsymbol{x},t) = div(\boldsymbol{B}\boldsymbol{B}^T(\boldsymbol{x})\nabla p_{T-1,0}(\boldsymbol{x},t) - 2k_f(N_b-T+1)p_{T-1,0}(\boldsymbol{x},t)\\ - k_b^s(T-1)p_{T-1,0}(\boldsymbol{x},t) + k_b^d p_{T-1,1}(\boldsymbol{x},t)\\ + k_f(N_b-T+2)p_{T-2,0}(\boldsymbol{x},t).\end{aligned}$$

For $s = T-1$ and $N_b - T > d > 0$, (no transition rate from $P_{T,d}$), then

$$\begin{aligned}\frac{\partial}{\partial t}p_{T-1,d}(\boldsymbol{x},t) = div(\boldsymbol{B}\boldsymbol{B}^T(\boldsymbol{x})\nabla p_{T-1,d}(\boldsymbol{x},t)) - 2k_f(N_b-T+1-d)p_{T-1,d}\\ - (k_b^s(T-1)+k_b^d d)p_{T-1,d}(\boldsymbol{x},t) + k_b^d(d+1)p_{T-1,d+1}(\boldsymbol{x},t)\\ + k_f(N_b-T-d+2)p_{T-2,d}(\boldsymbol{x},t)\\ + k_f(N_b-T-d+2)p_{T-1,d-1}(\boldsymbol{x},t).\end{aligned}$$

The CME at the threshold number of bound miRNAs ($s = T$)

For $s = T$ and $N_b - T > d > 0$ (the only transition occurs from the state T $-$ 1), then

$$\frac{\partial}{\partial t}p_{T,d}(\boldsymbol{x},t) = k_f(N_b-T-d+1)p_{T-1,d}(\boldsymbol{x},t).$$

The CME at the limit of a filled mRNA ($s + d = N_b$)

For $T > s > 0$ and $N_b - s = d$ (there are no transition rates from any state (s, d) such that $s + d > N_b$), then

$$\frac{\partial}{\partial t} p_{s,N_b-s}(\boldsymbol{x}, t) = div(\boldsymbol{B}\boldsymbol{B}^T(\boldsymbol{x})\nabla p_{s,N_b-s}(\boldsymbol{x}, t)) - (k_b^s s + k_b^d(N_b - s)) p_{s,N_b-s}(\boldsymbol{x}, t) + k_f p_{s-1,N_b-s}(\boldsymbol{x}, t) + k_f p_{s,N_b-s-1}(\boldsymbol{x}, t).$$

For $s = T$, $N_b - T = d$, then

$$\frac{\partial}{\partial t} p_{T,N_b-T}(\boldsymbol{x}, t) = k_f p_{T-1,N_b-T}(\boldsymbol{x}, t).$$

Finally, for $d = N_b$, $s = 0$ (the mRNA is filled with decoys), then

$$\frac{\partial}{\partial t} p_{0,N_b}(\boldsymbol{x}, t) = div(\boldsymbol{B}\boldsymbol{B}^T(\boldsymbol{x})\nabla p_{0,N_b}(\boldsymbol{x}, t)) - k_b^d d p_{0,N_b} + k_f p_{0,N_b-1}(\boldsymbol{x}, t).$$

Appendix B

MFPT to a small pore on the domain boundary

For the RNAi model, the general approximation of the MFPT, τ, of a Brownian mRNA particle initially located at the center of a spherical domain, of radius R, moving with diffusion coefficient, D, to hit one of $N \gg 1$ identical, circular pores, of radius ε, on the surface of the domain, is given in Singer et al. (2008) by

$$\tau \sim \frac{|\Omega|}{4\varepsilon DN}\left[1 - \frac{\varepsilon}{\pi}\log\varepsilon + \frac{\varepsilon N}{\pi}\left(\frac{1}{5} + \frac{4b_1}{\sqrt{N}}\right)\right] + \frac{R^2}{6D}. \tag{44}$$

The coefficient $b_1 \approx -0.5668$ is calculated by Cheviakov et al. (2010) by minimising the energy, $\mathcal{H}$, of the arrangement of the N traps across the surface of a unit sphere (i.e., $R = 1$). In (44), $\frac{R^2}{6D}$ represents the MFPT of a particle, initially located at the center of the spherical domain, to reach the surface. If $N\varepsilon \gg 1$, the time taken for a particle to locate a pore on the surface of the domain, i.e., the first term, will dominate over the time taken for the particle to reach the surface, i.e., the second term, which leads us to the approximation

$$\tau \sim \frac{|\Omega|}{4\varepsilon DN}\left[1 - \frac{\varepsilon}{\pi}\log\varepsilon + \frac{\varepsilon N}{\pi}\left(\frac{1}{5} + \frac{4b_1}{\sqrt{N}}\right)\right]. \tag{45}$$

MFPT to a small target within domain

We similarly compute the mean time for an mRNA to locate a ribosome in the *PTEN* problem as follows (Cheviakov et al. 2010, 2013) in the case of many traps: for N

uniformly distributed traps of radius $\varepsilon \ll 1$ in the interior of the spherical domain, Ω, of unit radius, R, with reflecting boundary, the MFPT, τ, of a Brownian particle uniformly distributed in the domain, moving with diffusion coefficient D, to a trap is given by

$$\tau \sim \frac{|\Omega|}{D}\left[\frac{1}{4\pi\varepsilon N c} + \frac{1}{N^2}\left(\frac{\mathcal{H}_{ball}}{4\pi} - \frac{7N^2}{10\pi}\right)\right]. \tag{46}$$

Here, $\mathcal{H}_{ball}$ (similar to $\mathcal{H}$ declared in the previous section) is defined as the energy function for optimising the spatial arrangement of the N traps within the spherical domain (typical values for varying N in a unit sphere are given in Table 2 of Cheviakov et al. 2011); and c is the normalized capacitance of each trap ($c = 1$ for a disk), assumed here to be the same for all traps (typical values for varying trap shapes are given in Table 1 of Cheviakov et al. 2011). For example, assuming there are $N = 10$ spherical traps of radius ε, we have $\mathcal{H}_{ball} = 243.37$ and $c = 1$. The narrow escape approximation is equivalent to replacing escape by a Poissonian event of rate $\frac{1}{\tau}$.

Forward binding rate of small RNA to a binding site on mRNA

The binding rate, k_f, of a diffusing particle to one of the N_b binding sites on an mRNA is the reciprocal of the MFPT to a site. When the sites, of size a, are located on a sphere of radius r, this MFPT is given in Cheviakov et al. (2010) as

$$\tau_N = \frac{1}{k_f} = \frac{|\Omega|}{D}\left(\frac{1}{4\pi r} + \frac{1}{4N_b a}\right). \tag{47}$$

References

Alberts B (1998) Essential cell biology: an introduction to the molecular biology of the cell. Garland

Alberts B, Johnson A, Lewis J, Raff M, Roberts K, Walter P (2008) Molecular biology of the cell, 5th edn. Garland Science, New York

Broderick JA, Salomon WE, Ryder SP, Aronin N, Zamore PD (2011) Argonaute protein identity and pairing geometry determine cooperativity in mammalian rna silencing. RNA 17(10):1858–1869

Cheviakov AF, Ward MJ, Straube R (2010) An asymptotic analysis of the mean first passage time for narrow escape problems: part ii: the sphere. Multiscale Model Simul 8(3):836–870

Cheviakov AF, Ward MJ (2011) Optimizing the principal eigenvalue of the laplacian in a sphere with interior traps. Math Comput Model 53(7–8):1394–1409

Cheviakov AF, Zawada D (2013) Narrow-escape problem for the unit sphere: homogenization limit, optimal arrangements of large numbers of traps, and the n^2 conjecture. Phys Rev E 87(4):042118

Dao Duc K, Holcman D (2010) Threshold activation for stochastic chemical reactions in microdomains. Phys Rev E 81(4 Pt 1):041107

Ebert MS (2010) Molecular titration by microRNAs and target mimic inhibitors. Ph.D. thesis, Massachusetts Institute of Technology

Ebert MS, Neilson JR, Sharp PA (2007) Microrna sponges : competitive inhibitors of small rnas in mammalian cells. Nat Methods 4(9):721–726

Eiring AM, Harb JG, Neviani P, Garton C, Oaks JJ, Spizzo R, Liu S, Schwind S, Santhanam R, Hickey CJ, Becker H, Chandler JC, Andino R, Cortes J, Hokland P, Huettner CS, Bhatia R, Roy DC, Liebhaber SA, Caligiuri MA, Marcucci G, Garzon R, Croce CM, Calin GA, Perrotti D (2010) Mir-328 functions as an rna decoy to modulate hnrnp e2 regulation of mrna translation in leukemic blasts. Cell 140(5):652–665

Gillespie DT (1977) Exact stochastic simulation of coupled chemical reactions. J Phys Chem 81(25):2340–2361

Grünwald D, Singer RH (2010) In vivo imaging of labelled endogenous β-actin mrna during nucleocytoplasmic transport. Nature 467(7315):604–607

Holcman D, Schuss Z (2004) Escape through a small opening: receptor trafficking in a synaptic membrane. J Stat Phys 117, 5/6(41):91–230

Holcman D, Schuss Z (2012) Brownian needle in dire straits: stochastic motion of a rod in very confined narrow domains. Phys Rev E 85:010103

Jackson R, Standart N (2007) How do microrna regulate gene expression? Sci STKE 2007 367:re1

Morozova N, Zinovyev A, Nonne N, Pritchard LL, Gorban AN, Harel-Bellan A (2012) Kinetic signatures of microrna modes of action. RNA 18(9):1635–1655

Paul CP, Good PD, Winer I, Engelke DR (2002) Effective expression of small interfering rna in human cells. Nat Biotechnol 20(5):505–508

Poliseno L, Salmena L, Zhang J, Carver B, Haveman WJ, Pandolfi PP (2010) A coding-independent function of gene and pseudogene mrnas regulates tumour biology. Nature 465(7301):1033–1038

Putz U, Howitt J, Doan A, Goh CP, Low LH, Silke J, Tan SS (2012) The tumor suppressor pten is exported in exosomes and has phosphatase activity in recipient cells. Sci Signal 5(243):ra70–ra70

Ragan C, Zuker M, Ragan MA (2011) Quantitative prediction of mirna-mrna interaction based on equilibrium concentrations. PLoS Comput Biol 7(2):e1001090

Robb GB, Brown KM, Khurana J, Rana TM (2005) Specific and potent rnai in the nucleus of human cells. Nat Struct Mol Biol 12(2):133–137

Salmena L, Carracedo A, Pandolfi PP (2008) Tenets of pten tumor suppression. Cell 133(3):403–414

Schuss Z, Singer A, Holcman D (2007) The narrow escape problem for diffusion in cellular microdomains. Proc Natl Acad Sci 104(41):16098–16103

Schuss Z (2010) Diffusion and stochastic processes: an analytical approach. Springer series on applied mathematical sciences, 170. Springer, New York

Singer A, Schuss Z, Holcman D (2008) Narrow escape and leakage of brownian particles. Phys Rev E 78(5):051111

Sumazin P, Yang X, Chiu HS, Chung WJ, Iyer A, Llobet-Navas D, Rajbhandari P, Bansal M, Guarnieri P, Silva J, Califano A (2011) An extensive microrna-mediated network of rna-rna interactions regulates established oncogenic pathways in glioblastoma. Cell 147(2):370–381

Tay Y, Kats L, Salmena L, Weiss D, Tan SM, Ala U, Karreth F, Poliseno L, Provero P, Di Cunto F, Lieberman J, Rigoutsos I, Pandolfi PP (2011) Coding-independent regulation of the tumor suppressor pten by competing endogenous mrnas. Cell 147(2):344–357

Usmani RA (1994) Inversion of a tridiagonal jacobi matrix. Linear Algebra Appl 212–213:413–414

Vargas DY, Raj A, Marras SAE, Kramer FR, Tyagi S (2005) Mechanism of mrna transport in the nucleus. Proc Natl Acad Sci 102(47):17008–17013

Xiao C, Srinivasan L, Calado DP, Patterson HC, Zhang B, Wang J, Henderson JM, Kutok JL, Rajewsky K (2008) Lymphoproliferative disease and autoimmunity in mice with increased mir-17-92 expression in lymphocytes. Nat Immunol 9(4):405–414